UNCLASSIFIED

(2)

AD-A243 726

CUMENTATION PAGE

Form Approved
OMB No. 0704-0188

1. AGENCY USE ONLY (Leave blank)	2. REPORT DATE	3. REPORT TYPE AND DATES COVERED
	October 23, 1991	Final Report 6/15/89 - 12/15/91

4. TITLE AND SUBTITLE

(U) Study of Turbulence by Photon Correlation Spectroscopy

5. FUNDING NUMBERS

PE - 61102F
PR - 2307
SA - BS
G - AFOSR 89-0415

6. AUTHOR(S)

W I Goldburg

7. PERFORMING ORGANIZATION NAME(S) AND ADDRESS(ES)

+ Department of Physics and Astronomy
++ Department of Mechanical Engineering
University of Pittsburgh, Pittsburgh, PA 15260

8. PERFORMING ORGANIZATION REPORT NUMBER

AFOSR-TR- 91 0996

9. SPONSORING/MONITORING AGENCY NAME(S) AND ADDRESS(ES)

AFOSR/NA
Building 410
Bolling AFB DC 20332-6448

10. SPONSORING/MONITORING AGENCY REPORT NUMBER

AFOSR-89-0415

11. SUPPLEMENTARY NOTES

12a. DISTRIBUTION/AVAILABILITY STATEMENT

Approved for public release; distribution is unlimited

12b. DISTRIBUTION CODE

13. ABSTRACT (Maximum 200 words)

We have studied grid-generated turbulence in a water tunnel at moderate Reynolds numbers. The method used was the standard one of Laser Doppler Velocimetry (LDV) and an novel scheme, which we call photon homodyne correlation spectroscopy(HCS). With LDV, we measured the probability density function of velocity differences $P(\delta v(\ell))$ on varying spatial scales ℓ, by invoking the frozen turbulence hypothesis. The HCS technique permits measuring P without using this hypothesis. Of special interest to us was the behavior of the system at and above a Reynolds number (Re_c) where the turbulence becomes self-similar, in that $< \delta v(\ell)^2 > \sim \ell^{\zeta}$. Above Re_c the exponent ζ increases from 0 to 2/3 with increasing Re.

91 1 127

14. SUBJECT TERMS

Turbulence, light scattering, scaling

15. NUMBER OF PAGES

37

16. PRICE CODE

17. SECURITY CLASSIFICATION OF REPORT	18. SECURITY CLASSIFICATION OF THIS PAGE	19. SECURITY CLASSIFICATION OF ABSTRACT	20. LIMITATION OF ABSTRACT
Unclassified	Unclassified	Unclassified	UL

This research was a study of grid-generated turbulence by a novel method of photon homodyne correlation spectroscopy (HCS). The scheme enables one to measure velocity differences $V(R)$ on a spatial scale R, with no need to invoke the Taylor's frozen turbulence hypothesis. In this work we compared such measurements with with Laser Doppler Velocimetry measurements of the velocity at a point, $v(t)$. From the latter experiment, we deduced the velocity difference $V(R)$ with the Taylor assumption, $R = \delta t/U$, where U is the mean flow velocity and δt is the time interval between velocity measurements.

In that work it was observed that the time-time averaged velocity difference, $< V(R) >$, was of self-similar form, $< V(R) >= aR^{\zeta}$, where ζ is a function of Re, and a is a constant, which was also measured. The AFOSR support enabled us to build a much larger tunnel and to span a wider range of Reynolds numbers. Before summarizing our new results, I describe the HCS measuring scheme in elementary terms.

If a light beam strikes a single particle moving with velocity $\mathbf{v}$, the frequency of the light is shifted by an amount $\mathbf{k} \cdot \mathbf{v}$, where $\mathbf{k}$ is the the scattering vector of the light. If the scattering angle with respect to the incident beam is θ, then the magnitude of $\mathbf{k}$ is $(4\pi/\lambda)sin(\theta/2)$, where λ is the wavelength of light. This frequency shift is the basis for laser Doppler Velocimetry (LDV). If now, the incident beam strikes two particles, moving with velocities $\mathbf{v_1}$ and $\mathbf{v_2}$, and if the scattered light falls on a photomultiplier, the output of this device will be a photo-current modulated at the beat frequency $\mathbf{k} \cdot \vec{\mathbf{v}}_1 - \mathbf{kv_2})$. Thus, one has a measurement of the <u>difference</u> in velocity of the two particles. This is the basis of HCS.

It turns out that one can measure velocity differences even when the beam traversing the turbulent fluid is scattered by a large number of particles. In this case, the beatings of Doppler shifts from many particle pairs, causes the scattered intensity, I(t), to fluctuate in time. These temporal fluctuations can be measured by a frequency analyzer, or more conveniently, by measuring the intensity correlation function, $< I(t')I(t'+t) >$, where the brackets designate an average over t'. If one images the scattered light beam on a slit of adjustable width L, then the (normalized) intensity correlation function $< I(t')I(t'(t) > / < I(t') >^2 >\equiv g(t)$, has the form,

$$g(t) = 1 + \int_0^L b(R)d(R) \int_{-\infty}^{\infty} P(V(R))cos(kV(R))dV(R) = 1 + G(t), \qquad (1)$$

where $b(R) = (2/L)(1 - R/L)$ is the number fraction of seed particles separated by a distance R, in the slit, and $P(R)$ is the probability density function for velocity differences on a scale (R). The symbol, $V(R)$ denotes the projection of the velocity difference $\mathbf{V}(R)$ along the direction of the scattering vector $\mathbf{k}$.

We note several features of the above equation. The cosine factor is just the beat frequency associated with velocity differences $V(R)$, coming from particle pairs. Because the speed of light is so very large, the experiment effectively measures simultaneously, velocity difference from the particles constituting a pair (It turns out that the scattering from triplets of particles, etc, average to zero). Hence the Taylor hypothesis need not be invoked. In principle a knowledge of $P(R)$ is sufficient to determine all the moments of $V(R)$, from which the spectrum of fractal exponents can be extracted - if indeed the turbulent energy lies on a fractal or multifractal. In practice, one cannot measure the higher moments of $P(R)$ with the HCS scheme, but one can learn a lot about the functional form of $P(R)$. Because the direction of the incident and scattered beams are at the experimenters disposal, velocity differences $\mathbf{V}(R)$ can be measured in any direction, so the presence or absence of isotropy of the turbulence can be determined. Like LDV, the HCS scheme is non-invasive.

This grant enabled us to construct a rather fine tunnel, roughly 10 cm × 10 cm in cross section. An important feature of this tunnel was that its flat walls were of optical quality, so that the scattering vector was well defined, and a sharp image could be formed on the slit. The mesh size M of the grid in this new tunnel was 0.85 cm. The grant also enabled me to buy a laser Doppler velocimeter, so that it was possible to compare the results of the HCS and LDV measurements at the same point in the turbulent stream, namely 21 cm down stream from the grid.

In the LDV measurements we concentrated on measuring the probability density of velocity differences $P'(V(R))$, so that this function could be compared with the HCS measurements of $P(V(R))$ introduced above. If the Taylor hypothesis were applicable, P and P' would be equal, assuming, of course that the values of R were the same in both experiments. It turns out that the HCS scheme is most suited for studying velocity differences in small scales, R, whereas the LDV scheme yielded the most accurate information at large values of R. Nevertheless, the overlap interval of the two measuring schemes was significant, namely 0.5 mm < R < 2.5 mm. With the present optics we probe eddies as small as 0.1 mm with HCS, the limitation being the width to which we can focus the beam segment which is imaged on the slit.

We have found that if Re exceeds some critical value, which we call Re_c, the probability density $P(V(R))$ has the simple scaling form, $P(V(R)/u(R))$, where $u(R)$ is the characteristic width of P. Over a decade in R, this width varies algebraically with R, i.e., $u(R) \sim R^{\zeta(Re)}$. In the Kolmogorov theory, the exponent $\zeta = 1/3$. We find, on the other hand, that this exponent increases from approximately zero to 1/3 as Re is increased above Re_c. At our largest achievable values of Re, $\zeta \simeq 1/3$. One interpretation of this observation is that the turbulence is increasing from sheet-like (fractal dimension $D = 2$) to volume-filling (D=3) as Re is increased. In quite independent experiments, carried out in a different way, Sreenivasan and his students have come to the same conclusion.

From a measurement of $G(t)$ one can, in principle, deduce $P(V)$ using Eq. 1. One sees from that equation that P is closely related to the Fourier transform of $G(t)$. In practice it is often difficult to determine a function from its experimentally measured Fourier transform, and thus it was here. All we can say is that we can recover the measured $G(t)$ with a P that is the product of Gaussian and Lorentzian factors, i.e.

$$P(R) = const \cdot exp(-V(r)/2u'(R)^2) \times 1/(V(R)^2 + u(R)^2), \qquad (2)$$

with $u'(R)$ roughly five times $u(R)$. This large ratio implies that, in the range of our measurements, P departs only slightly from Lorentzian form. The LDV measurements are also consistent with a $P(R)$ of the above form, but in this case u and u' are almost equal. The measurements leave no doubt that, in the domain of eddies sizes R and Reynolds numbers probed by these experiments, the time

domain measurements (LDV) and the space domain measurements (HCS) yield very different forms for $P(V)$. Almost all existing measurements of this probability density are made in the time domain, with the spatial information extracted by invoking the Taylor hypothesis. Recently Sreenivasan has taken some measurements, using a single hot wire annemometer and also a pair of them. He too finds a failure of the frozen turbulence assumption. This past week I will give an invited colloquium at Yale and had an opportunity to compare notes with him.

I have summarized the work completed under the AFOSR grant. The experiments in our water tunnel are continuing, and we are also probing the transition from chaos to turbulence in a couette cell. We are also exploring the possibility of measuring the probability density for the vorticity, $P(\omega(R))$ by optical means. The completed work has resulted in a number of publications, as you see in the addendum. In addition I have been invited to present our results at various meetings, both in the US and abroad. Professor Sirivat, Professor Tong, Mr. Pak and I are very grateful for the support we have received from the AFOSR. The work done under this grant constitutes the PhD thesis of Mr. Pak.

ADDENDUM

List of of publications that came from the AFOSR support:

1. "A Light Scattering Study of Turbulence", (W. I. Goldburg, P. Tong, and H. K. Pak), Physica D 38 (1989) 134-140.
2. "Scaling Laws in Weak Turbulence", (with H. K. Pak, W. I. Goldburg and P. Tong), (in press).
3. "An Experimental Study of Weak Turbulence", (with H. K. Pak and W. I. Goldburg), "Fluid Dynamics Research" (in press).
4. "Measuring the Probability Distribution of the Relative Velocities in Grid-Generated Turbulence" H.K. Pak, and W.I. Goldburg, (submitted for publication).

Invited talks that are an outgrowth of this work:

1. International Conference on Fractals in Physics
   (A conference in honor of B. Mandelbrot), Nice, 1989.
2. SIAM Conference on Turbulence, Orlando, May, 1990.
3. Gordon Conference on Fractals, Plymouth NH, August, 1989.
4. International Workshop on Novel Experiments and Data Processing
   for Basic Understanding of Turbulence, Tokyo, October, 1990.
5. Program on Spatially Extended Nonequilibrium Systems, Santa Barabara,
   Aug. 1992.

APPENDIX A

A Light Scattering Study of Turbulence

by W J Goldburg, P Tong, and H K Pak

Physica D 38 (1989) 134–140
North-Holland, Amsterdam

A LIGHT SCATTERING STUDY OF TURBULENCE

W.I. GOLDBURG, P. TONG [1] and H.K. PAK
Department of Physics and Astronomy, University of Pittsburgh, Pittsburgh, PA 15260, USA

By scattering light from a turbulent fluid seeded with small particles, one obtains information about turbulent velocity fluctuations over varying spatial scales, R. The measured intensity autocorrelation function, $g(t)$, is related to the probability density $P(V(R))$ of finding velocity fluctuations of magnitude $V(R)$ associated with eddies of size R. The measurements described here strongly suggest that the energy-containing eddies occupy a fractal region whose dimension (or spectrum of dimensions) increases with the Reynolds number Re when Re exceeds some threshold value.

1. Introduction

In his seminal book, The Fractal Geometry of Nature, Benoit Mandelbrot [1] makes clear his deep interest in the geometrical nature of turbulence. As he points out, the description of the visual appearance of a turbulent fluid, such as smoke curling up from a cigarette, taxes our powers of description. It seems that present-day speech is not well suited to evoking the image of self-similar structures. After all, it takes a series of images, one magnified with respect to the other, to identify fractal structures. And turbulence is, by all evidence, a fractal thing at its roots [2].

There are many ways of revealing the fractal or spotty nature of a turbulent fluid. One technique is to measure the time variation of the square of the velocity at a point in the fluid [3]. Another is to add a small amount of long-chain molecules to the fluid and observe it through crossed polaroids [4]. The molecules are locally aligned by turbulent shear forces. These molecules, being anisotropic scatterers, depolarize the light in regions where the shear is large, making the local structure of the strong vorticity directly visible.

Herein we describe experiments, carried out at the University of Pittsburgh, which provide a new approach to the study of the small-scale structure of turbulence. The method involves a measurement of the autocorrelation function of the light intensity scattered by small particles suspended in the turbulent fluid. For this technique there is no need to invoke the "frozen turbulence assumption" to translate temporal information to spatial information. According to this assumption, small-scale eddies (the ones of interest), are transported past a velocity measuring device with the mean velocity U of the flow. If these small-scale eddies remain intact for a long enough time, a time record of the velocity $v(t)$ at a point will reveal spatial features of the flow through the equation $v(t)=v(x/U)$. The frozen turbulence assumption fails unless the velocity fluctuations $V(R)$ associated with eddies of size R are uncoupled from the larger-scale eddies.

The technique of photon correlation homodyne spectroscopy (HS) [5], which we have used in our experiments, is that of recording the beating of scattered light waves that have been Doppler shifted by pairs of particles seeded in the turbulent fluid. The technique was introduced many years ago by Bourke et al. [6], but seems largely to have been ignored. Being an optical technique, it permits non-invasive observation of velocity fluctuations at very small scales.

The homodyne scheme is readily understood from

[1] Present address: Exxon Research and Engineering Co., Annandale, NJ. 08801, USA.

Essays in honour of Benoit B. Mandelbrot
Fractals in Physics – A. Aharony and J. Feder (editors)

fig. 1, which shows two moving particles at a particular instant of time when their separation is R and their velocities are v_1 and v_2. The seed particles are small enough that they scatter light isotropically. A photodetector (PMT), located at an angle θ with respect to the incident beam, receives the light from both particles. The scattered light from each particle is Doppler shifted by an amount $\boldsymbol{k}\cdot\boldsymbol{v}_1$ and $\boldsymbol{k}\cdot\boldsymbol{v}_2$ respectively, where $\boldsymbol{k}$ is the scattering vector, of magnitude $k=(4\pi n/\lambda)\sin(\frac{1}{2}\theta)$. Here λ is the vacuum wavelength of the light ($\lambda=488$ nm in our experiments), and n is the refractive index of the turbulent fluid; in our case the fluid was water. The photomultiplier, which receives the light from the particle pair, is a square-law detector, so that its output current, $I(t)$, contains a beating term proportional to $\cos[kV_k(R)t]$, where V_k is the projection of the velocity difference v_1-v_2 along the direction of $\boldsymbol{k}$. Henceforth the subscript on $V_k(R)$ will be dropped, but its R dependence will be retained.

The essential aspect of turbulence is that the velocity difference between two points in the fluid depends on the separation R of these two points. According to the theory of Kolmogorov [6], the moments of the velocity fluctuations $V(R)$ obey a scaling law

$$\langle V(R)^n\rangle \sim u(R)^n \sim R^{\xi_n}, \tag{1}$$

with $\xi_n=\frac{1}{3}n$. The homodyne technique is well suited to measure the lower moments of $V(R)$, but not the higher moments. On the other hand, the method yields information about the functional form of the probability density $P(V(R))$, that two points in the fluid, separated by a distance R, have velocity difference lying within $V(R)$ and $V(R)+\mathrm{d}V(R)$. Our central finding is that $P(V(R))$ is well represented by a Lorentzian function,

$$P(V(R))\propto\{1+[V(R)/u(R)]^2\}^{-1}, \tag{2}$$

for relatively small values of $V(R)$. We also find that the scaling velocity $u(R)\sim R^{\zeta}$, where ζ is a function of Reynolds number, Re. The measurements were made at very modest values of the Reynolds number. In fact the turbulence was so weak that one might not have thought the flow would exhibit the self-similarity which was indeed observed. Throughout this paper the Reynolds number is defined as $\mathrm{Re}=Ul_0/\nu$, where U is the mean velocity of the flow, l_0 is the outer scale of the turbulence, and ν is the kinematic viscosity of the fluid.

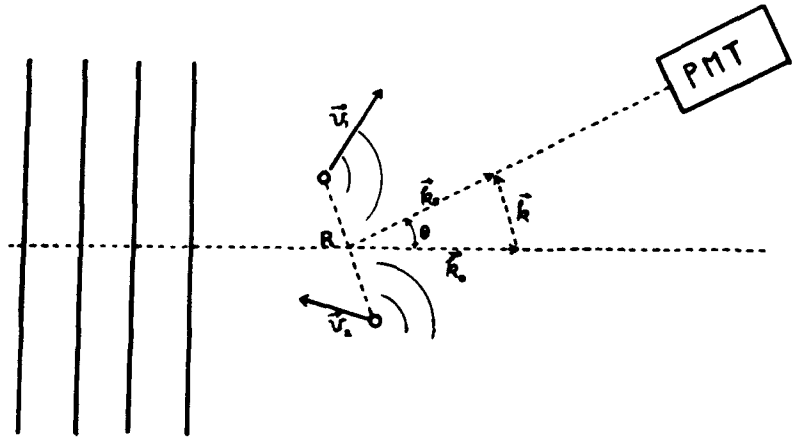

Fig. 1. A schematic diagram showing scattering geometry. The scattering vector $\boldsymbol{k}=\boldsymbol{k}_s-\boldsymbol{k}_0$, where $\boldsymbol{k}_s$ and $\boldsymbol{k}_0$ are the scattered and incident wave vectors respectively.

2. Experimental

The detailed experimental setup can be found in ref. [8]. The fluid flow was generated in a closed water tunnel comprised of a cylindrical pipe and a pump of variable speed. The turbulence is generated by a grid within the pipe. The grid can be removed to permit study of wall-generated turbulence (pipe flow). A baffle section placed in the high-pressure side of the grid, suppresses the turbulence generated by the pump and by those sections of pipe on the high-pressure side of the grid. With this arrangement all of the turbulence is generated by the grid only. In most of the experiments discussed here the diameter of the pipe was 4.4 cm, and the aperture size of the grid was 3.1 mm. These parameters are taken to be l_0 in calculating the Reynolds number. The measurements were made 28 cm downstream from the grid. The water which flowed through the pipe was seeded with polystyrene spheres 60 nm in diameter. These particles were small enough to scatter light isotropically and in sufficient concentration that their mean separation was much less than the Kolmogorov dissipation length l_d, which was estimated to be a fraction of a millimeter.

On the downstream side of the grid there is an optically transparent section of piping to admit the incident laser beam and observe the scattering. Because the flow is seeded, a thin column of the scattered light is produced in the water and that light is imaged with a lens, on a slit of variable width, L. By varying L, the homodyne scheme permits the probing of velocity fluctuations $V(R)$ from the smallest scale l_d to that of the width of the slit, L.

Using a standard light scattering apparatus and a digital correlator, we measure the intensity autocorrelation function, $g(t)=\langle I(t')\,I(t'+t)\rangle/\langle I(t')\rangle^2$, where $I(t)$ is the scattered light intensity measured at scattering angle θ, and the angle brackets represent a time average over t'. One can show [8] that the correlation function $g(t)$ has the following form:

$$g(t)=1+f(A)\,G(t)\,. \tag{3}$$

The geometrical factor $f(A)$ is of order unity if the photodetector receives light from only one coherence area [5]. All of the interesting physics is contained in $G(t)$, which is proportional to a sum of the time-averaged phase factors $\cos(ktV)$ coming from the Doppler shift of all particle pairs in the scattering volume. The function $G(t)$ can be written as [8]

$$G(t)=\int_0^L \mathrm{d}R\,h(R)\int_{-\infty}^{\infty}\mathrm{d}V(R)\,P(V(R))\,\cdot\,\times\cos[kV(R)t]\,, \tag{4}$$

where $h(R)$ is the probability of finding a particle pair, separated by R, in the columnar region of length L.

If the image on the slit is taken to be quasi-one-dimensional, which is valid when the slit width remains large compared to the diameter of the laser beam, $h(R)=2(1-R/L)/L$. Note that the inner integral in eq. (4) is the Fourier cosine transform of $P(V(R))$, and the $G(t)$ may be thought of as a transform of the characteristic function. If the probability density $P(V(R))$ has the scaling form $P(V(R))=Q[V(R)/u(R)]/u(R)$, eq. (4) becomes

$$G(t)=\int_0^L \mathrm{d}R\,h(R)\,F(ktu(R))\,. \tag{5}$$

where F is the Fourier cosine transform of $Q[V(R)/u(R)]$. It is easy to show that the scaling law in eq. (1) follows if the probability density function $P(V(R))$ has the above mentioned scaling form.

The above equations for $g(t)$ have quite general validity. They hold, for example, even if the fluid is stationary, and the seed particles are undergoing Brownian motion only. In that case, $V(R)$ is independent of R and $P(V(R))$ is a Gaussian function. Then the function $G(t)$ is an exponentially decaying function [5], $G(t)=\exp(-2Dk^2t)$, where D is the diffusivity of the Brownian particles, and is given by Stokes' law. This contribution to the decay of $G(t)$ will be present, even when the fluid is turbulent. However, in a turbulent fluid, the decay time T of $G(t)$ is much shorter than the diffusive decay time, $T_d=1/2Dk^2$, so that the latter contribution can be

safely ignored. From eq. (5), it follows that the turbulent decay time should be of the order of $T = 1/ku(L)$, because the fastest decay rate is associated with the largest eddies of size L.

3. Results

Over a wide range of slit widths and Reynolds numbers, we find that the function $G(t)$ exhibits the scaling form,

$$G(kt, L, \mathrm{Re}) = G(\kappa) , \qquad (6)$$

with $\kappa \sim k^{\mu} L^{\zeta} t$. This scaling behavior of $G(t)$ is observed only when the Reynolds number exceeded a certain value Re_c. In the case of the grid flow described above, Re_c was roughly 500, which corresponds to much weaker turbulence than that one normally associates with scaling behavior. It is quite possible that the scaling behavior is seen at such small values of Re because the simultaneous velocity difference $V(R)$ is measured and no frozen turbulence assumption is needed in the data analysis.

The exponent μ in eq. (6) was measured as follows. For a fixed slit width L and a fixed Re, $G(t)$ was measured at several scattering angles and hence several values of k. All of the plots of $\log[G(t)]$ versus $\log(t)$ could be superimposed by horizontal translation of one graph with respect to another. The amount of translation, $\delta(k)$, is found to be roughly proportional to k, i.e. $\mu = 1$, when Re exceeded the critical value Re_c. However, in the absence of flow, $\mu = 2$, as expected for Brownian motion of the seed particles. Similar measurements were made in which k and Re were held fixed, and L was varied. Again all the plots of $\log[G(t)]$ versus $\log(t)$ could be superimposed, yielding the result $\kappa \sim kL^{\zeta} t$, as long as Re exceeded Re_c. In these experiments, ζ is found to be Re dependent. We return to this important observation below.

Fig. 2, a log–log plot of $G(\kappa)$ versus κ, shows the scaling behavior of $G(t)$ discussed above. The measurements correspond to several values of scattering angle, or k-value, several slit widths and at various

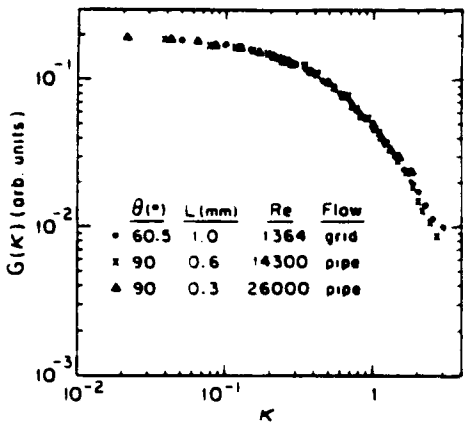

Fig. 2. The scaling function $G(\kappa)$ versus $\kappa = qu(L)t$ in pipe flow and grid flow.

Reynolds numbers. In one set of measurements (closed circles), the grid was present; in the other two sets (crosses and triangles), the grid was removed (pipe flow). The correlation functions $G(t)$ have been horizontally (and vertically) translated so that they coincide. In the pipe flow measurements, the Reynolds number is based on the pipe diameter, making it an order of magnitude larger than that for the grid flow, even when the mean flow velocities U are comparable in both cases.

An alternative way to determine the exponent ζ was to plot, on a double logarithmic scale, the slit-width dependence of the decay time, T, of $G(t)$, keeping Re and k fixed. As is shown in fig. 3, linear variation of $\log(T)$ with $\log(L)$ was seen at intermediate values of L. The data in fig. 3 were obtained in the grid flow at three different Reynolds numbers Re = 460, 1400, and 2200. Since $T \approx 1/ku(L)$ and $u(L) \sim L^{\zeta}$, the slope of this line yields the exponent ζ, which is 1/3 in the Kolmogorov theory. We have verified that the power law behavior at large L was limited by the outer scale, l_0, of the turbulence. At small values of L the beam diameter was no longer negligibly small, which could account for the decrease in T at small values of L. Imperfections in the optical system may also be responsible for the decrease in T at small slit widths.

The behavior of $T(L)$ at small L has more recently been reexamined in a water tunnel of much superior

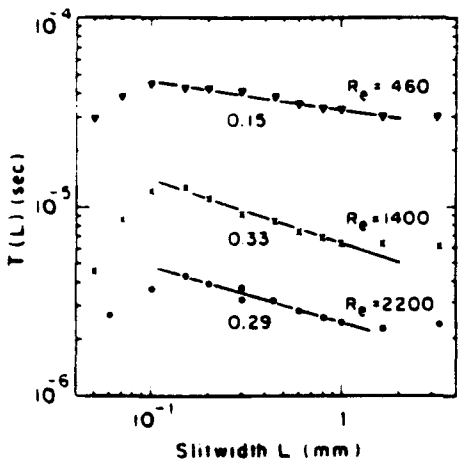

Fig. 3. The decay time $T(L)$ versus slit width L in grid flow. The number below a line is the slope of that line.

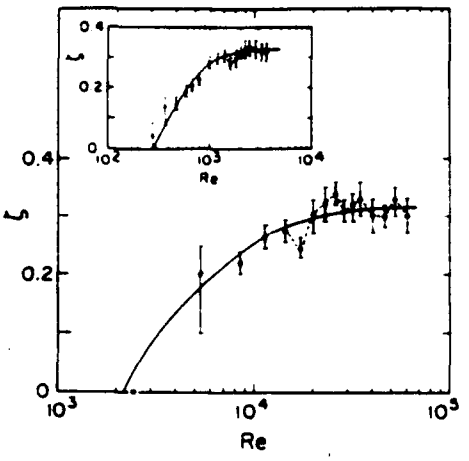

Fig. 4. The exponent ζ as a function of Re in pipe flow. The solid line is drawn by eye through the data points, and the dashed curve shows the oscillatory behavior of ζ. The inset shows ζ versus Re in grid flow.

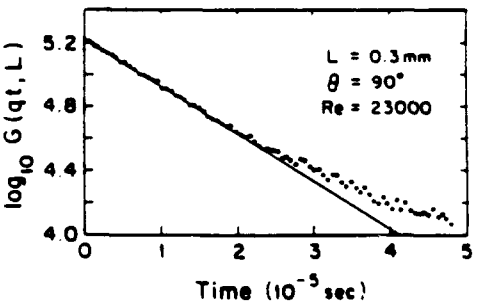

Fig. 5. A plot of $\log[G(qt, L)]$ versus t in pipe flow at indicated parameters.

design to that used in the studies reported above. In this experiment, the optically transparent pipe, where $g(t)$ was measured, was square in cross section, rather than cylindrical, so that the laser beam was undistorted in passing through it. In this square pipe, the beam diameter was less than 0.1 mm, which is smaller than the smallest value of L at which $g(t)$ was measured. Using laser Doppler velocimetry and invoking the frozen turbulence assumption one can determine the smallest eddy size l_d. At Re = 850, we obtained $l_d = 0.4$ mm. At values of L between 0.4 mm ($= l_d$) and 0.1 mm, the decay time of $G(t)$ became independent of L, i.e. $\zeta \approx 0$ when $L < l_d$. This result is very different from the Kolmogorov prediction, $\zeta = 1$ when $L < l_d$.

From the straight-line segment (solid line in fig. 3) we can extract the slope ζ which shows a Re-dependent feature. Fig. 4 shows ζ as a function of Re for both pipe flow and grid flow (insert). The exponent ζ is seen to increase from 0 to $\approx 1/3$ (the Kolmogorov value) as Re is increased. When the Reynolds number is below Re_c, $G(t)$ fails to exhibit scaling behaviour. The measured $Re_c \approx 300$–400 in the grid flow and $Re_c \approx 3000$–4000 when the grid was removed. Measurements in the improved water tunnel give similar results. These observations are consistent with the notion that the turbulence becomes increasingly three-dimensional as Re is increased above Re_c and that in the vicinity of Re_c, the turbulence is two-dimensional [9].

We now turn to the discussion about the functional form of $G(t)$. Fig. 5 is a semilog plot of $G(t)$ versus t in pipe flow at the indicated values of L, θ, and Re. The straight line is a linear fit to the data points at small t. It is seen that only at large time does the curve start to deviate from the linear behavior. If we assume that the characteristic function $F(ku(R)t)$ in eq. (5) has the form $F \sim \exp[-ku(R)t]$, $G(t)$ then

becomes an incomplete gamma function with $ku(L)t$ as its argument [8]. This equation is well fitted to our measurement of $G(t)$. An example of this good fit is shown in fig. 6. Note that the assumption of $F(x)$ being a single exponential decaying function implies that $P(V(R))$ is of Lorentzian form as shown in eq. (2). This function has a diverging second moment, to which the energy density in the fluid is proportional. Therefore $G(t)$ cannot have this form for large values of $V(R)$. We indeed observed departures from this Lorentzian form for $P(V(R))$ with very large values of $V(R)$ (corresponding to very small t for $G(t)$) [10,11]. However, these observations will not be discussed further here. Most theories of turbulence concentrate on the scaling behavior of the moments of $V(R)$, rather than in $P(V(R))$ itself. Quite often, $P(V(R))$ is assumed to be of Gaussian form, $P(V(R)) \sim \exp\{-[V(R)/u(R)]^2\}$, but this form of $P(V(R))$ is clearly contrary to our findings.

How can one understand that the exponent ζ increases from 0 to $\approx 1/3$ as the fluid becomes increasingly turbulent? A fundamental understanding of this result is lacking, but it can be said that the observation is consistent with the notion that the turbulent active region is a fractal [12]. Let the fractal dimension of the turbulent region be D. Since the turbulent energy is confined to active regions of dimension $D<3$, the concentration of the turbulent energy is increased to smaller regions, relative to the case of volume-filling turbulence. Modifying the Kolmogorov theory to take this effect into account [13], one has $u(R) \sim R^{\zeta}$, with $\zeta = \frac{1}{3}(1+D-3)$. According to this model, the increase of ζ from 0 to $\approx \frac{1}{3}$ corresponds to an increase of D from 2 to 3.

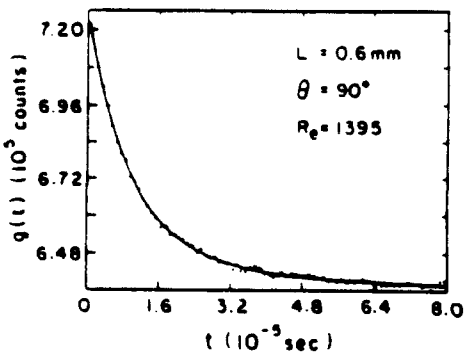

Fig. 6. A typical autocorrelation function $g(t)$ versus t in grid flow. The solid line is a fit to the incomplete gamma function.

It should be stressed that our measurements of $g(t)$ described above, do not directly give information about the fractal dimension of the energy-containing eddies; it can only be said that the data invite such an interpretation. The above interpretation of the data in fig. 4 is supported by the recent work of Shreenivasan et al. [3]. They measured the fractal dimension of the interface of two counter-flowing fluids, one of which has been dyed. Such measurements, made in the vicinity of Re_c, support the conclusion that increasing Re above Re_c increases the dimensionality of the turbulent active region. With one adjustable parameter, Re_c, the data of Shreenivasan et al. can be directly superimposed on the measurements in fig. 4 [3].

Even if the energy-containing eddies in a turbulent field occupy regions with dimensionality less than 3, it is not necessary that the entire turbulent region be characterized by a homogeneous fractal. Benzi et al. [14] have proposed a model that the turbulent region is a multifractal object. In their model there is a probability, x, that the turbulent region is space filling ($D=3$) and a probability, $1-x$, that $D=2$. Our measurements are consistent with this model, provided one makes an additional assumption that x is a function of the Reynolds number. The details of the model have been worked out for a general function of $x(\mathrm{Re})$ and fitted to experiment [9]. At present, however, our measurements are not precise enough to confirm that a multifractal model is required to explain the observations.

4. Concluding remarks

What started out as a study carried out in the time domain (the measurement of $g(t)$), has ended up by yielding spatial information about turbulent flow. The homodyne experiments provide further confirmation of the notion of Mandelbrot that the energy-

containing eddies are fractal in their geometrical structure. This finding is not new. What seems to have gone unnoticed before, is that the fractal dimension of the turbulence changes with changing Reynolds number, when some critical value of this parameter is exceeded. The interpretation of these experiments makes no appeal to the frozen turbulence assumption. By using the technique of photon correlation homodyne spectroscopy, we have been able to observe the self-similar behavior of turbulent flows at moderate Reynolds number that were heretofore regarded as too weak to exhibit universal features.

Acknowledgements

We have benefited from illuminating discussions and correspondence with K.R. Shreenivasan, M. Nelkin, and J. Stavans and have enjoyed a continuing fruitful interaction with A. Onuki. We are grateful for the collaboration of our colleague, A. Sirivat and to C.K. Chan for his essential contributions in the early stages of this work. This research was supported by the National Science Foundation under Grant No. DMR-8611666.

References

[1] B.B. Mandelbrot, The Fractal Geometry of Nature (Freeman, San Francisco, 1982).
[2] B. Mandelbrot, Phys. Fluids Suppl. 10 (1967) S302.
[3] K.R. Sreenivasan, R. Ramshankar and C. Meneveau, Proc. Roy. Soc. (London) A 421 (1989) 79.
[4] E.R. Lindgren, Arch. Fys. (1959) 97.
[5] B.J. Berne and R. Pecora, Dynamic Light Scattering (Wiley, New York, 1976).
[6] P.J. Bourke et al., J. Phys. A 3 (1970) 216.
[7] A.N. Kolmogorov, C.R. (Dokl.) Acad. Sci. URSS 30 (1941) 301; 31 (1941) 538.
[8] P. Tong et al., Phys. Rev. A 37 (1988) 2125;
P. Tong and W.I. Goldburg, Phys. Fluids 31 (1988) 2841.
[9] P. Tong and W.I. Goldburg, Phys. Fluid 31 (1988) 3253.
[10] A. Onuki, Phys. Lett. A 127 (1988) 143.
[11] P. Tong and W.I. Goldburg, Phys. Lett. A 127 (1988) 147.
[12] B.B. Mandelbrot, J. Fluid Mech. 62 (1974) 331; in: Lecture Notes in Physics, Vol. 12, Statistical Models and Turbulence, M. Rosenbblatt and C.W. Van Atta, eds. (Springer, Berlin, 1972), p. 333.
[13] U. Frisch, P. Sulem and M. Nelkin, J. Fluid Mech. 87 (1978) 719.
[14] R. Benzi et al., J. Phys. A 17 (1984) 3521.

APPENDIX B

Scaling Laws In Weak Turbulence

by H K Pak, W I Goldburg, and P Tong

SCALING LAWS IN WEAK TURBULENCE

H. K. PAK[†], W. I. GOLDBURG[†] and P. TONG[‡]

[†] Department of Physics and Astronomy
University of Pittsburgh, Pittsburgh, PA 15260

[‡] Department of Physics
Oklahoma State University, Stillwater, Oklahoma 74078

ABSTRACT. Photon Homodyne Spectroscopy (HCS) and Laser Doppler Velocimetry (LDV) have been used to study turbulent velocity fluctuations $V(R)$ associated with eddies of size R. For small R both types of measurement were consistent with a model in which the active regions of turbulence lie on a fractal of dimension D, with D increasing from ~ 2 to ~ 3 as the Reynolds number (Re) increases above some threshold value. At larger eddy sizes, the LDV measurements show a different scaling of the velocity fluctuations. We associate these larger eddies with the energy reservoir that feeds the inertial cascade.

INTRODUCTION

It is known that the motion of an incompressible fluid is regular and smooth at low Reynolds number (Re). As Re increases, the flow becomes chaotic and irregular, and finally it develops into turbulence. One of the essential aspects of turbulence is that the large-scale eddies which initially contain most of the kinetic energy, split into smaller scale eddies, and the process is repeated, again and again, until the size of the eddies is so small that their kinetic energy dissipates into heat. Elementary theories of fully developed turbulence are based on the hypothesis that the small scale statistics of turbulent flow obeys universal scaling properties, such as

$$V^n(R) \sim R^{hn}, \tag{1}$$

where $V(R)$ is the velocity difference associated with turbulent eddies of size R. In general, $h \approx 1/3$ for fully developed turbulence (Kolmogorov 1941).

We describe experiments in which the above self-similarity is observed in a weakly turbulent grid flow, even though the maximum Reynolds numbers reached in these experiments is not very large. This self-similarity or scaling was seen in two different ways: homodyne photon correlation spectroscopy (HCS) and laser Doppler velocimetry (LDV).

TECHNIQUES

With the LDV technique (Durrani and Greated 1977) the Doppler shifted light scattered by small particles suspended in the turbulent fluid is mixed with the reference

beam. The detected light intensity $I(t)$ is therefore modulated by the Doppler frequency, $\mathbf{q} \cdot \mathbf{v}(\mathbf{r}, t)$, where $\mathbf{q}$ is scattering vector and $\mathbf{v}(\mathbf{r}, t)$ is the local velocity of scatterers in the fluid. Our interest in the LDV measurement was focused on the variance,

$$< V^2(\tau) > \equiv < |v(t' + \tau) - v(t')|^2 > . \quad (2)$$

To relate $< V^2(\tau) >$ to the spatial velocity variation, $< V^2(R) >$, we used Taylor's hypothesis (frozen turbulence assumption) which assumes $R = U\tau$, where U is the mean flow velocity.

With the HCS technique (Berne and Pecora 1976, Tong et al. 1988), one measures the intensity correlation function $g(t) = < I(t'+t)I(t') >$. If one normalizes $g(t)$ so that $g(t) = 1 + const \cdot G(t)$, with $G(0) = 1$ and $G(\infty) = 0$, then

$$G(t) = \int_0^L h(R)\, dR \int_{-\infty}^{\infty} dV(R)\, P(V(R), R) cos(qV(R)t). \quad (3)$$

Here, $V(R)$ is the component of the instantaneous velocity difference $\mathbf{V}(R)$ along the scattering vector $\mathbf{q}$, and $P(V(R). R)$ is its probability density function. The scattering volume viewed by a photodetector is assumed to be quasi-one-dimensional with length L, and $h(R) = 2(1 - R/L)/L$ is the probability density of finding a pair of particles separated by a distance R in the scattering volume. Equation (3) means that the light scattered by each pair of particles contributes a phase factor $cos(qV(R)t)$ (due to the frequency beating) to the intensity correlation function $g(t)$, and $g(t)$ is the incoherent sum of these ensemble averaged phase factors over all the particle pairs in the scattering volume.

EXPERIMENTAL

The fluid flow was generated in a closed water tunnel with a variable speed pump. Undesirable flow disturbances produced by the pump and piping system were damped out in the plenum chamber on the high pressure side of the grid. The grid, which generates the turbulence, consists of an array of rods of width $0.016\,cm$ and with a mesh size, $M = 0.85\,cm$. The Reynolds number is defined as $Re = UM/\nu$, where ν is the kinematic viscosity of water.

The tunnel itself (Pak et al. 1991) is $110\,cm$ long and its square cross section is $10\,cm \times 10\,cm$. Polished plexiglass windows are furnished on four sides of the water tunnel to admit the incident laser beam and to observe the scattering. A recovery tank is located at the low pressure end of the tunnel. Its large volume slows the flow before the water returns to the pump intake. The water was distilled and seeded with polystyrene spheres of uniform size. These particles scatter the light for both the HCS and LDV measurements. The observation point for both experiments was on the axis of the tunnel and $21\,cm$ down stream from the grid, where the spanwise velocity profile is flat. All measurements were made at room temperature.

In the HCS experiment a mildly focused argon-ion laser beam entered the test section from above, and the scattering measurements were made in the horizontal plane. A lens was placed in such a position as to form an 1:1 image in the plane of an adjustable slit. It is the slit width L which controls the scattering volume size viewed by the photomultiplier. For the LDV measurement we used standard techniques for measuring the stream-wise component of the velocity $v_x(t)$. The Taylor's hypothesis is expected to be valid only if the rms velocity fluctuations around the

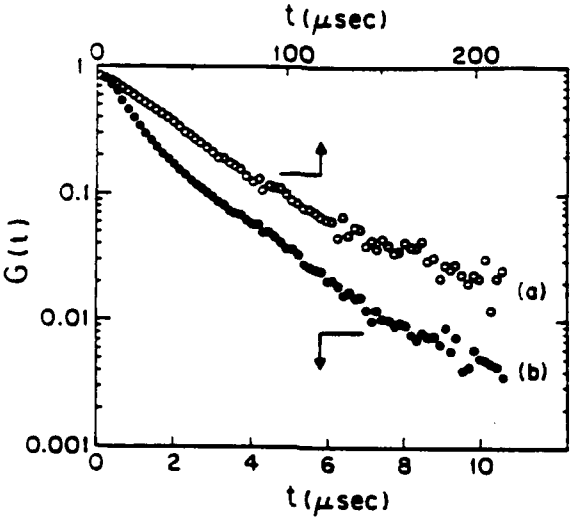

Figure 1. Measured $G(t)$'s for (a) the turbulent grid flow of $Re = 1800$ and $L = 0.7\,mm$ and (b) turbulent Couette flow of $Re = 8.3 \times 10^5$ and $L = 1.0\,mm$.

mean, $\sqrt{< (v_x(t) - U)^2 >}$, are small compared to U itself. For all the measurements reported here, $\sqrt{< (v_x(t) - U)^2 >}/U$ was less than 4%.

RESULTS

In the HCS measurement, it was found that over a limited range of slit widths and Reynolds numbers, $G(t)$ has the scaling form, $G(t) \propto G(qu(L)t)$. Figure 1(a) shows a typical $G(t)$ in the water tunnel. Here Re is 1800 and the slit width is $0.7mm$. We define $u(L)$ from the inverse of the decay time of $G(t)$, i.e. $1/T = qu(L)$. Therefore $u(L)$ is the characteristic turbulence velocity difference at length scale L. The above scaling form of $G(t)$ was seen only when Re exceeded some critical value, $Re_c \simeq 300$. It was also found that $u(L)$ has a scaling form, $u(L) \sim L^{\alpha}$. As Re increases from $Re \simeq 300$ to 800, α increases from 0 to 1/3 (the Kolmogorov value), and beyond $Re \simeq 800$. α saturates at the value of 1/3 (see Fig. 2(a)). The minimum usable value of L is limited by the laser beam width to $0.2\,mm$. The upper limit of L was set by optical coherence effects (Berne and Pecora 1976) to approximately $0.2\,cm$.

Figure 3 is a *log-log* plot showing a typical $< V^2(R) >$ *vs* R of LDV, subtracting R-independent contributions from the instrumental phase fluctuations (Pak et al. 1991). These measurements were made at $Re = 330$ (curve (a)) and $Re = 1400$ (curve (b)) respectively. The curves have been shifted vertically to improve visibility. In the LDV measurements the smallest R was limited by the scattering volume size $0.3\,mm$, and in the opposite limit of R is approximately the mesh size, $M = 0.85\,cm$. For $Re \gtrsim 300(Re_c)$, there are two scaling regimes in which $< V^2(R) > \sim R^{\zeta}$ for $R \lesssim 0.15\,cm$ and $< V^2(R) > \sim R^{\eta}$ for $R \gtrsim 0.15\,cm$. Curves (b) and (c) of Fig. 2 are scaling exponents $\zeta/2$ for small R and $\eta/2$ for large R respectively. For small R,

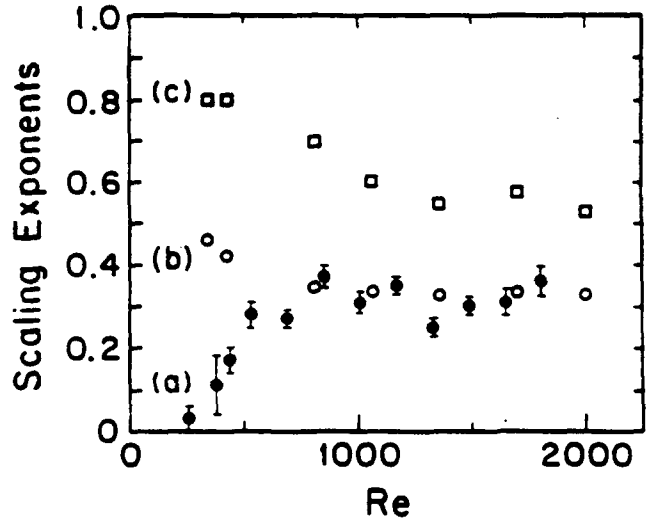

Figure 2. Scaling exponents in the inertial subrange and the energetic subrange measured by LDV and by the HCS techniques: (a) $\alpha(Re)$ in the inertial subrange measured by HCS. (b) $\zeta/2(Re)$ in the inertial subrange measured by LDV. (c) $\eta/2(Re)$ in the energetic subrange measured by LDV.

where both techniques probe overlapping ranges of R, as α increases from 0 to 1/3. $\zeta/2$ decreases from 1/2 to 1/3. Both exponents, α and $\zeta/2$ saturate at 1/3 for $Re \gtrsim 800$. For large R, as Re increases, $\eta/2$ decreases from 0.8 and saturates at 0.5. Below we offer a possible explanation as to why α and ζ should vary oppositely with increasing Re.

DISCUSSION

To interpret the LDV and HCS measurements at small R, we invoke the β model (Mandelbrot 1976, Frisch et al. 1978). According to this model the turbulent kinetic energy in the inertial range lies in an "active" region having fractal dimension D. With this model $P(V(R), R)$ can be factorizable to the form. $P^*(u(R), R) \cdot R^{3-D}$. Here $P^*(u(R), R)$ is the probability density of $u(R)$ in the active region and the factor R^{3-D} is proportional to the sparcity of active turbulent regions at small R. Therefore the product of R^{3-D} and $h(R)$ is proportional to the probability of finding a particle pair in an active region within the slit. These factors have little effect on $u(R)$. For this reason, an HCS experiment of $u(L)$ is a measurement of velocity differences in the active regions of the turbulence only. From this model one readily derives that $\alpha = (D-2)/3$. Therefore an increase of α from 0 to 1/3 implies that D is increasing from 2 to 3.

The LDV technique for small R, unlike HCS, probes both the "active" and "inactive" regions of the flow, since both regions are moved past the observation point at the mean flow speed U. Because of the sparcity of active turbulent regions, $< V^2(R) > \sim u^2(R) \cdot R^{3-D} \sim R^\zeta$ with $\zeta = 1-\alpha = (5-D)/3$. Accordingly, $\zeta/2$ should

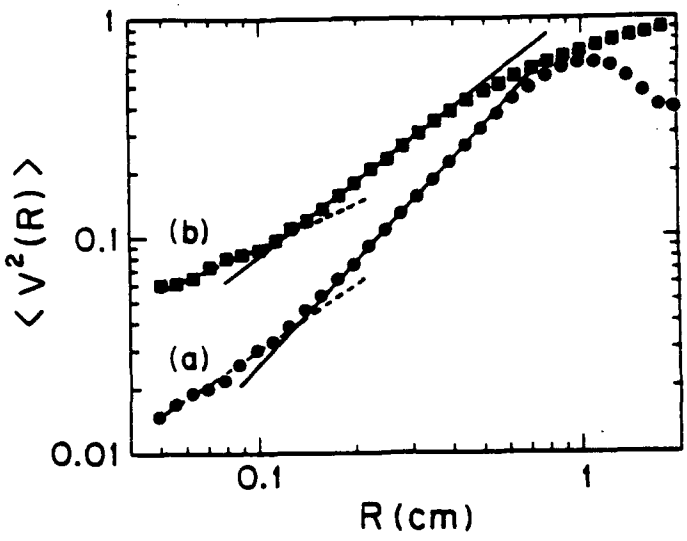

Figure 3. *Log-log* plot of $< V^2(R) >$ vs R from the LDV measurements. Shown here are measurements at $Re = 1400$ (a) and $Re = 330$ (b). The dashed and solid lines, of slope $\zeta/2$ and $\eta/2$ respectively, are discussed in the text.

decrease from 1/2 to 1/3 as α increases from 0 to 1/3. The small-R range (inertial range), where the above fractal model can be applied, is limited from below by the Kolmogorov dissipation scale. The inertial-range eddies are fed by a reservoir of larger, energy-containing eddies which normally are not associated with self-similarity. Nevertheless the measurements of $< V^2(R) >$ at large R (the solid lines of Fig. 2 and curve (c) in Fig. 3) seem to define an exponent (η) associated with these energy-containing eddies. Since the range of R where η is well defined is much less than a decade, $\eta(Re)$ may have little physical meaning.

Recently we have commenced HCS measurements in a flow between two concentric cylinders (Couette Cell), with the inner one rotating (Tong et al. 1990). When this flow was highly turbulent, $G(t)$ (and by implication of $P(V(R), R)$) was clearly of different functional form than for the water tunnel measurements. Curve (b) of Fig.1 is $G(t)$ for the Couette flow at $Re = 8.3 \times 10^5$ and slit width $L = 1mm$ when the laser beam passed through the gap radially.

CONCLUSION

The combined LDV and HCS experiments reported here provide additional evidence that in the inertial range of eddy sizes, the fractal dimension D of the turbulence increases with increasing Reynolds number. The observations are consistent with an increase in D from ~ 2 to ~ 3 as Re increases above some system-dependent threshold value, Re_c. This assertion is based on the recognition that these two measurement schemes average over the velocity fluctuations $V(R)$ in different ways. The HCS technique probes the active region only, whereas the LDV measurements average over the inactive regions as well.

ACKNOWLEDGEMENTS

The authors have profited from a fruitful collaboration with Anuvat Sirivat and Preben Alstrom. This work has been supported by grants from the Air Force Office of Scientific Research, No. P6784, and from the National Science Foundation, No. DMR-8914351.

REFERENCES

Berne, B. J. and R. Pecora (1976) Dynamic Light Scattering, (John Wiley & Sons).

Durrani, T. S. and C. A. Greated (1977) Laser Systems in Flow Measurement, (Plenum Press, New York).

Frisch, U., P. Sulem and M. Nelkin (1978) 'A Simple Dynamical Model of Intermittent Fully Developed Turbulence', J. Fluid Mech, 87, 719-736.

Kolmogorov, A. N. (1941) A. N. C. R. Acad. Sci. USSR 30, 301-358.

Mandelbrot, B. (1976) 'In Turbulence and Navier-Stokes equation', in R. Temam (eds.), Lecture Notes in Math. 565, Springer, 121.

Pak, H. K., W. I. Goldburg and A. Sirivat (1991) 'An Experimental Study of Weak Turbulence', Fluid Dyn. Res. (to appear).

Tong, P., W. I. Goldburg, C. K. Chan and A. Sirivat (1988) 'Turbulent Transition by Photon Correlation Spectroscopy', Phys. Rev. A 37, 2125-2133.

Tong, P., W. I. Goldburg, J. S. Huang and T. A. Witten (1990) 'Anisotropy in Turbulent Drag Reduction', Phy. Rev. Lett. 65, 2780-2783.

APPENDIX C

Measuring the Probability Distribution of the Relative Velocities in Grid-Generated Turbulence

by H K Pak and W I Goldburg

Version July 17

Measuring the Probability Distribution of the Relative Velocities in Grid-Generated Turbulence

H. K. Pak and W. I. Goldburg

Department of Physics and Astronomy, University of Pittsburgh, Pittsburgh, PA, 15260

A. Sirivat

Department of Mechanical Engineering, University of Pittsburgh, Pittsburgh, PA 15261

Homodyne photon correlation spectroscopy (HCS) and laser Doppler velocimetry (LDV) were used to study the probability density function of velocity differences $\delta v(\ell)$ between points in the fluid separated by a distance ℓ. These two measuring schemes yield different results for the probability density, $P(\delta(v(\ell))\, d\delta v(\ell)$. Both types of measurement show that $P(\delta v(\ell))$ is well approximated by the product of Gaussian and Lorentzian factors, with P being more Lorentzian-like for the HCS measurements and more Gaussian-like for the LDV measurements. The HCS method probes the spatial fluctuations directly, whereas the LDV technique records temporal fluctuations in velocity and relates them to the spatial fluctuations through the Taylor hypothesis.

PACS numbers: 47.25.Ae, 47.25.Cg

In turbulent flow the quantity of interest is not so much the velocity itself, $\mathbf{v}(\mathbf{r},t)$, as the instantaneous difference in velocity at two points separated by a distance ℓ. This quantity $\delta\mathbf{v}(\ell) \equiv v(\mathbf{r}+\ell,t) - \mathbf{v}(\mathbf{r},t)$ is characterized by a probability density function, $P(\delta v(\ell))\, d\delta v(\ell)$, where v is the measured component of $\mathbf{v}$. Herein we report measurements of $P(\delta v(\ell))$ in turbulent flow generated by a grid in a water tunnel. The experiments explore a range of ℓ-values and span a range of Reynolds numbers under conditions that possibly lie between chaotic behavior and fully developed turbulence.

Our measurements of $P(\delta v(\ell))$ will be compared with a measured probability density function $P'(\delta v(\ell))$ deduced from a record of the velocity as a function of time, recorded at a single point in the turbulent fluid. Both types of measurement were made at almost exactly the same position in the turbulent stream. To deduce spatial information from the time record of the the velocity, it is necessary to invoke the so-called Taylor hypothesis (frozen turbulence assumption) [1], which simply means that $v(t)$ is replaced by $v(x/U)$ where U is the mean flow velocity. Virtually all measurements of the probability density function for velocity differences on scales ℓ have been made in this way [2]. It is this probability density which we have designated as P'.

In the work reported here, P and P' are found to be very different. As for P, it is well represented by the product of Gaussian and Lorentzian terms. The Lorentzian factor is found to have a much smaller width, $u_L(\ell)$, than the width $u_G(\ell)$, of the Gaussian factor. The new measurements reported substantiate those made in a much smaller water tunnel [3–5]. The function P' is much more Gaussian in form than P, but it too gives a heavier weighting to large velocity fluctuations than does a purely Gaussian function or even an exponential one. If one parameterizes P' by the product of Gaussian and Lorentzian factors, the widths of these two factors are comparable in magnitude. For our measurement at least, the frozen turbulence assumption fails,

i.e, P and P' are conveying different information [6].

The schemes for measuring P' and P are laser Doppler velocimetry (LDV) and homodyne photon correlation spectroscopy (HCS), respectively. The former technique is a standard one [7], whereas the HCS method has been used only recently [3, 8–11]. Both of these methods require the seeding of the fluid with small particles which follow the local flow and scatter light. The HCS method is sensitive to velocity differences rather than the velocity itself, because it registers the beating of Doppler shifts coming from pairs of particles moving relative to each other [3]. As will be discussed below, the optical scheme used here records velocity differences for all values of ℓ from the smallest eddy size present out to a size L, which is the width of a slit through which the light passes before it reaches the photodetector. Because one measures a scattered intensity rather than a scattered electric field, the HCS method yields information about the symmetric part of the probability density only. It is this part of the full probability density function that we label as $P(\delta v(\ell))$. Past measurements of P' in highly turbulent flows show that this function is not always symmetric [12, 13]. In the present LDV measurements $P'(\delta v(\ell))$ is also asymmetric, though the asymmetry is small.

Our HCS measurements of $P(\delta v(\ell))$ show it to be well approximated by the product of Lorentzian and Gaussian functions only if the Reynolds number of the flow, Re, exceeds some critical value, $Re_c \simeq 300$. Here we define Re as $Re = aU/\nu$, where a is the mesh size of the grid ($a = 8.5$ mm) and ν is the kinematic viscosity of water ($0.01\, cm^2/sec$). The widths of the Lorentzian and Gaussian factors are explicitly defined by the equation,

$$P = \frac{exp(-u_L(\ell)^2/2u_G(\ell)^2)}{\pi\, erfc(u_L(\ell)/\sqrt{2}u_G(\ell))} \cdot exp(\delta v(\ell)^2/2u_G(\ell)^2) \cdot \frac{u_L(\ell)}{\delta v(\ell)^2 + u_L(\ell)^2}, \qquad (1)$$

The ratio of these widths, $M \equiv u_G(\ell)/u_L(\ell)$ is found to be approximately 4. This

ratio is only weakly dependent on ℓ and Re in the range of parameters probed in this work namely, $0.3\,mm < L < 2.5\,mm$, $300 < Re < 1800$.

As discussed below, the quantity actually measured with the HCS scheme is the intensity correlation function, $g(t)$, of light scattered by the seed particles. This function is observed to have a self-similar form, which it would not have unless both widths, $u_L(\ell)$ and $u_G(\ell)$ are proportional to ℓ^h, with a common value of the exponent h. In this experiment, as in the earlier work, using a smaller water tunnel, h is observed to increase with increasing Re from $h \simeq 0$ to $h \simeq 1/3$, the Kolmogorov value [14].

The experiments were carried out in the water tunnel that was $10\,cm \times 10\,cm$ in cross section and 1.1 m in length. The measurements were made at an axial point 25 cm downstream from the grid. The spanwise profile of the flow was flat, making the time-averaged velocity gradient at the measuring point for P and P' ignorably small [11].

The water was seeded with polystyrene particles (diameter= $0.106\,\mu$), that were small enough to follow the local flow. The light source was the mildly focused beam from an argon ion laser operating the wavelength $\lambda = 488$ nm. The incident beam travelled perpendicular to the flow direction. The scattered light was detected in a direction that was also perpendicular to the flow. The incident beam traced out a clearly visible thin line in the flowing water, the diameter of this beam being less than 0.1 mm. The scattered light, at a scattering angle $\theta = 90°$, was imaged at 1:1 magnification on a slit of adjustable width L. This width is a crucial parameter in the experiment because it determines the maximum measurable eddy size, $\ell = L$, to which $g(t)$ is sensitive. More than $1.5\,m$ behind the slit was a photomultiplier which recorded the scattered intensity, $I(t)$. The output of the photomultiplier is a train of identically shaped pulses which are sent to the correlator, whose output is

the intensity correlation function $g(t) = < I(t'+t)I(t') > / < I(t') >^2$.

Under approximations which are well satisfied in these experiments, one can show [3] that $g(t)$ is given by

$$g(t) = 1 + A(t) \int_0^L b(\ell) d\ell \int_{-\infty}^{\infty} P(\delta v(\ell)) cos(k\delta v(\ell)t) d\delta v(\ell)) = 1 + G(t), \qquad (2)$$

where the scattering vector k is of magnitude $k = 2nk_o sin(\theta/2)$, and $\delta v(\ell)$ is the component of δv(ℓ) along the direction of k. The refractive index of the scattering medium (water) is $n = 1.33$. Quite generally, $G(t)$ is a decaying function, its characteristic decay time that is of the order of $1/ku(L)$, where $u(L)$ is the characteristic velocity difference over a slit width L. The function $b(\ell) = (2/L)(1-\ell/L)$ is the probability that a pair of particles, separated by ℓ, are to be found in the slit [3, 11]. This form of $b(\ell)$ is correct only if L is much greater than the beam diameter [3, 8]. The factor $A(t)$ represents the Brownian diffusion of the seed particles and takes account of the fact that even in the absence of turbulent flow, $G(t)$ will decay slowly and is of the form $A(t) \sim exp[-2Dk^2]$, where D is the diffusion constant. This parameter is determined from the diameter of the seed particle and the viscosity of water [15]. All of the experimental data have been corrected for this Brownian motion factor [11].

According to Eq. (2), if $P(\delta v(\ell))$ has the simple scaling form $P(\delta v(\ell)) = Q(\delta v(\ell))/u(\ell))$, and if $u(\ell) \sim l^h$, then $G(t)$ has the scaling form, $G(k, t, L) = G(x)$, where $x = ku(\ell)t$. Therefore a plot of $log\, G(t)$ vs $log\, t$, for fixed Re but various values of L, should produce curves, all of which should be superimposable when translated along the time axis. This is indeed what was observed in the earlier experiments [3] and in the present ones. Figure 1 shows $G(t)$ measured at the three slit widths $L =$ 0.5 mm, 1.1 mm, and 2 mm, the Reynolds number being $Re = 1490$. The function $G(t)$ has been normalized so that it approaches unity in the limit $t \to 0$ and zero as $t \to \infty$. Having confirmed that P is self-similar, we now examine its functional form.

Figure 2 is a semi-log plot of $G(t)$ at Re= 1490, L = 1.3 mm. Also shown is the best fit to Eq. (2), assuming that P is purely Gaussian ($P = [1/\sqrt{2\pi}u_G(\ell)]\, exp(-\delta v(\ell)^2/2u_G(\ell)^2)$) (solid line), and purely Lorentzian ($P = u_L(\ell)/\pi[u_L(\ell)^2 + \delta v(\ell)^2]$) (broken line). These two lines correspond to $u_L(L) = u_G(L) = 0.216\, cm/sec$. Variation of these parameter could not produce a good fit to these data with either the Gaussian or Lorentzian probability density function, though the Lorentzian fit is clearly superior. An exponential form for P is even more at odds with our observations, though it is observed in other experiments [12]. We have shown a Gaussian form for $P(\delta v(\ell))$ because it is sometimes observed for large values of ℓ [16]. A probability density of dominantly Lorentzian form gave a satisfactory fit to the measurements in Ref. [4]. We defer a discussion of other suggested and observed forms of $P(\delta v(\ell))$.

To proceed further we take note of the fact that the cosine factor in Eq. (2) implies that $G(t)$ must approach the origin with zero slope ($G(t) \sim 1 - const.t^2$), even though experimental limitations on the electronics bar an unambiguous observation of this behavior. We therefore attempted the fit to $G(t)$ with the product of a Lorentzian and a Gaussian function, the widths of these factors being adjustable parameters. As seen in the inset of Fig. 2 (solid line), it was possible to obtain a very good fit to the data with this form of P. A similarly good fit with this form of $G(t)$ was obtained at all values of L and Re. For each of the parameter pairs, $u_G(\ell)$ and $u_L(\ell)$, we have evaluated $M(\ell, Re)$ and find it to be approximately 4, increasing slightly with decreasing slit width (At Re = 1490, M = 2.7 at L = 1.3 mm, and M = 3.6 at L = 0.5 mm). There is no discernable trend with changing Re. Similar values of M were obtained in Ref. [4]. Onuki [17] has suggested that these two widths characterize velocity fluctuations inside and outside of the active regions. Abundant experiments suggest that the active regions of the turbulent dissipation lie on a fractal

or multi-fractal [18].

It is instructive to compare our measurements of $G(t)$ with a prediction that P is a log-normal distribution, since this functional form of P has a credible theoretical basis and many experiments have been aimed at testing the log-normal theory [2, 16, 19]. Here we compare our measurements with a modified log-normal theory due to Castaing et al. [13]. This theory, which is free of an inconsistency contained in the original log-normal theory [2], successfully explains recent measurements of the temperature-difference density function $P(\delta T(\ell))$ as measured in Rayleigh Benard convection by the Chicago group [20]. Castaing assumes that $\delta v(\ell)$ has a Gaussian distribution with variance $u(\ell)$, but that $u(\ell)$ is a random variable with a log-normal distribution. The specific form of P is

$$P_\lambda(\delta v(\ell)) = \int_0^\infty exp(-\delta v(\ell)^2/2u^2)\, exp(-ln^2(u/u(\ell))/2\lambda^2) du/u^2, \qquad (3)$$

where $u(\ell)$ is the most probable variance of $\delta v(\ell)$ and λ is the variance of $ln\, u$. To compare this prediction with our measurements, we assume that $u(\ell)$ may be taken to be the measured value of $u_L(L)$ (since the Lorentzian factor dominates in $G(t)$). The parameter, λ, is taken to have the form proposed by Castaing, namely $\lambda = (\ell/\ell_o)^\beta$, with $\beta = 0.24$. The parameter ℓ_o is set equal to the grid size of $8.5\, mm$. Inserting the above expression for P into Eq. (2) yields a $G(t)$ which is plotted as the broken line in the inset of Fig. 2. We note that a log normal form of P, such as in Eq. (3), assures that $G(t)$ will not have the self-similar form so clearly seen in Fig. 1. With the above values of β and $u(\ell)$, the log-normal theory is clearly not a good fit to the data in Fig. 2.

Next we turn to the LDV measurements of $P'(\delta v(\ell))$. With the LDV technique, the seed particles traverse optical interference fringes, modulating the intensity of the scattered light received by the photomultiplier. A commercially available counter-

signal conditioner records the frequency of these pulses and hence determines $v(t)$ at the observation point. The Taylor hypotheses is then invoked to convert the $v(t)$ into a temporally fluctuating signal, $v(x)$, where x is a coordinate in the flow direction [7]. The Taylor hypothesis is generally assumed to be valid when the ratio f of the rms fluctuations in the velocity about its mean value, U, is a small fraction of U itself. This condition was well satisfied in the present experiments where f was always less than 0.04. By splitting up the time record, $v(t)$, into segments of equal length δt, and replacing δt by ℓ/U, we create an the ensemble of velocity differences, $\delta v(\ell)$, from which $P'(\delta v(\ell))\, d\delta v(\delta \ell)$ can be constructed with a histogram.

Fig. 3 is a semi-log plot of an LDV measurement of P' vs $\delta v(\ell)^2$ at $Re = 1490$ and $\ell = 1.3\, mm$. The solid line in the figure is a best fit to these data, assuming that P' is of the Lorentzian-Gaussian form of Eq. (1) (If P' were a Gaussian function, the data points would lie on a straight line in this figure). The parameters producing this fit are $u_L(L) = 0.32$ cm/sec and $u_G(L) = 0.47$ cm/sec, giving $M = 1.4$. This ratio is much smaller than M obtained from the HCS experiments. Those LDV measurements which spanned the same range of Re and L as the HCS experiments, could be fitted with a density function containing the product of Lorentzian and Gaussian factors. However, the exponent $h(Re)$ could not be determined without making questionable assumptions [11].

The broken line in Fig. 3 is the function P extracted from the HCS measurements made using the same values of Re and L as the LDV data in the figure. The parameters associated with this HCS measurement are $u_L(L) = 0.26$ cm/sec and $u_G(L) = 0.69$ cm/sec. Note that the Gaussian factor is weighted much more heavily than for the HCS measurements, i.e. M is smaller. The very different shape of the two curves in Fig. 3 leaves no doubt as to the failure of the frozen turbulence assumption here. Both P and P' give a greater weight to velocity fluctuations of large magnitude than

either a Gaussian or exponential function.

The failure of the frozen turbulence assumption indicates that the small-eddies, which are being probed here, do not maintain their geometrical shape as they are convected past the observation point at the mean velocity, U. A possible cause is the coupling between velocity fluctuations of many different sizes, a point that has received much theoretical attention [21, 22].

In summary, we have carried out measurements which expose the Taylor hypothesis (frozen turbulence assumption) to an experimental test and have measured the functional form of the probability density $P(\delta v(\ell))$ over a range of eddy sizes ℓ in the Reynolds number range 300 to 1800. The function P is well represented by the product of Gaussian and Lorentzian factors but not by either factor alone or by exponential or log-normal functions. These observations indicate the importance of probing turbulence in both the time and space domains.

ACKNOWLEDGMENTS

We have profited from discussions with P. Alstrom, K. Sreenivasan, P. Tong, and V. Yakhot. This work was supported by the National Science Foundation under Grant No. DMR-8914351.

REFERENCES

[1] J. L. Lumley, Phys. Fluids **8**, 1056 (1965).

[2] A. S. Monin and A. M. Yaglom, Statistical Mechanics(MIT Press, Cambridge, MA 1975), Vol. 2.

[3] P. Tong, W. I. Goldburg, C. K. Chan, and A. Sirivat, Phys. Rev. A **37**, 2125 (1988).

[4] P. Tong and W. I. Goldburg, Phys. Lett. **127**, 147 (1988).

[5] P. Tong and W. I. Goldburg, Phys. Fluids **31**, 2841 (1989).

[6] Preliminary measurements by K. Sreenivasan, in which both $v(t)$ and $\delta v(\ell)$ were measured, also indicate a failure of the Taylor hypothesis.

[7] L. E. Drain, The Laser Doppler Technique (John Wiley & Sons 1980).

[8] M. Ikegami and M. Shioji, Bull. JSME **29**, 2036 (1986).

[9] W. I. Goldburg, P. Tong, and H. K. Pak, Physica D **38**, 134 (1989).

[10] P. Tong, W. I. Goldburg, J. S. Huang, and T. A. Witten, Phys. Rev. Lett. **65**, 2780 (1990).

[11] H. K. Pak, W. I. Goldburg, and A. Sirivat, Fluid Dyn. Res. (in press) and references therein.

[12] F. Anselmet, Y. Gagne, E. J. Hopfinger, and R. A. Antonia, J. Fluid Mech. **140**, 63 (1984).

[13] B.Castaing, Y. Gagne and E. J. Hopfinger, Physica D **46**, 177 (1990).

[14] A. N. Kolmogorov, C. R. Acad. Sci. USSR **30**, 301 (1941).

[15] B. J. Berne and R. Pecora, Dynamic Light Scattering with Applications to Chemistry, Biology, and Physics (Wiley, 1976).

[16] C. Van Atta and J. Park, in "Statistical Models of Turbulence", edited by J. Ehlers, K. Hepp, and H. A. Weidenmuller (Springer Lecture Notes in Physics, Vol **12**, 1972) p. 402.

[17] A. Onuki, Phys. Lett. **127**, 143 (1988).

[18] K. R. Sreenivasan, Annu. Rev. Fluid Mech. **23**, 539 (1991).

[19] C. H. Gibson and P. J. Masiello, in "Statistical Models of Turbulence", edited by J. Ehlers, K. Hepp, and H. A. Weidenmuller (Springer Lecture Notes in Physics, Vol **12**, 1972) p. 427.

[20] F. Heslot, B. Castaing, and A. Libchaber, Phys. Rev. A **36**, 5870 (1987).

[21] V. Yakhot, S. A. Orzsag, and Z-S She, Phys. Fluids A **1**, 184 (1989).

[22] M. Nelkin and M. Tabor, Phys. Fluids A **2**, 81 (1990).

FIGURES

FIG. 1. Superimposed log-log plot of $G(t)$ for the three indicated slit widths, L and at the Reynolds number indicated.

FIG. 2. Semi-log plot of $G(t)$ at $Re = 1490$, $L = 1.3$ mm. The solid line is a Lorentzian fit to the data, and the broken line is a Gaussian fit. The characteristic widths $u_L(L)$ and $u_G(L)$ of both factors is 0.216 cm/sec. The inset shows the same data fitted to Eq. (1) (solid line) and to the log-normal model (broken line) discussed in the text.

FIG. 3. Semi-log plot of the probability density function as measured by laser Doppler velocimetry, the abscissa being $\delta v(\ell)^2$. The solid line is a fit to these data using Eq. (1) and the broken line is the function P extracted from the HCS measurements, using Eqs. (1) and (2). The measurements were at Re=1490 and ℓ =1.3 mm.

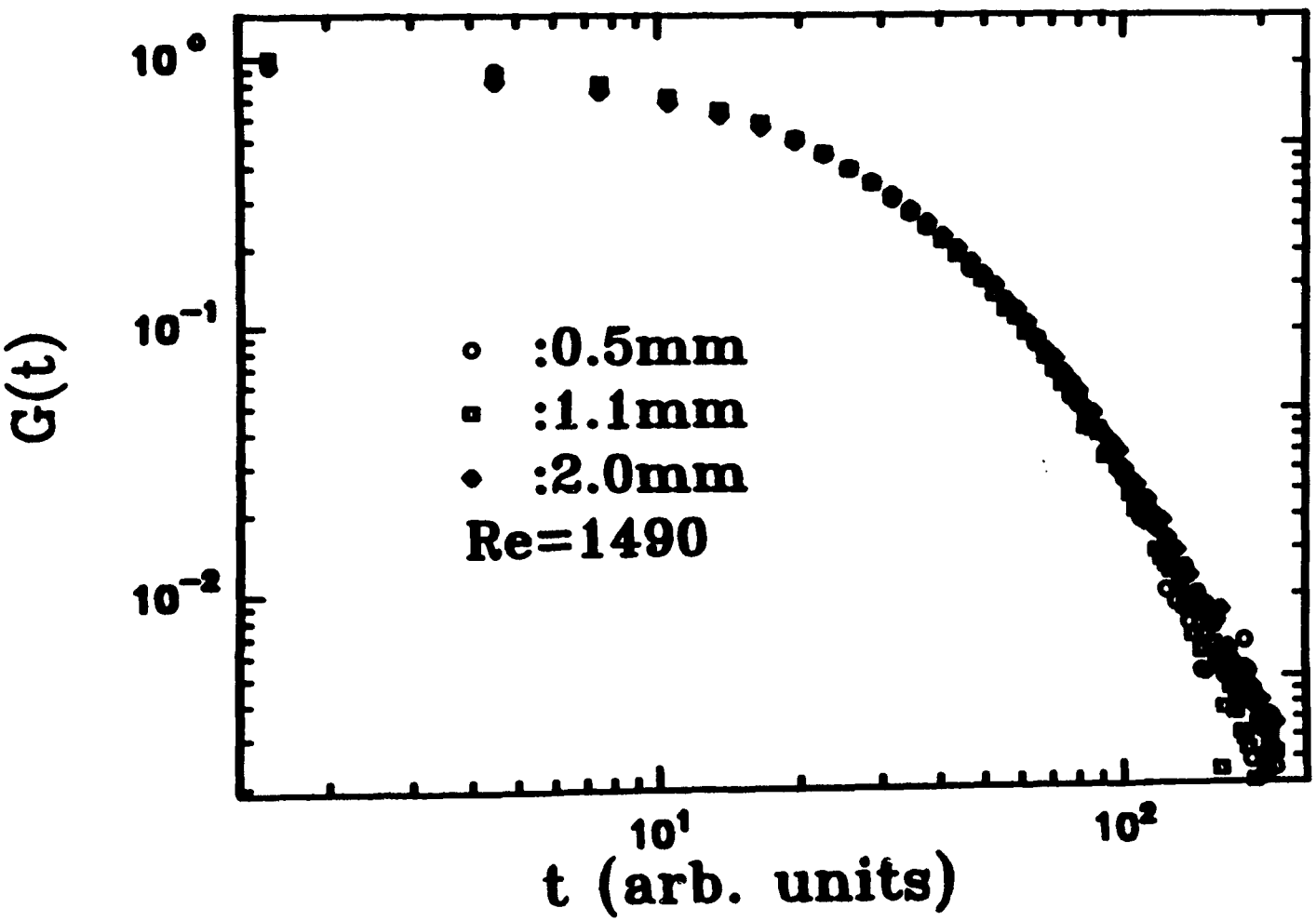

Fig 1.

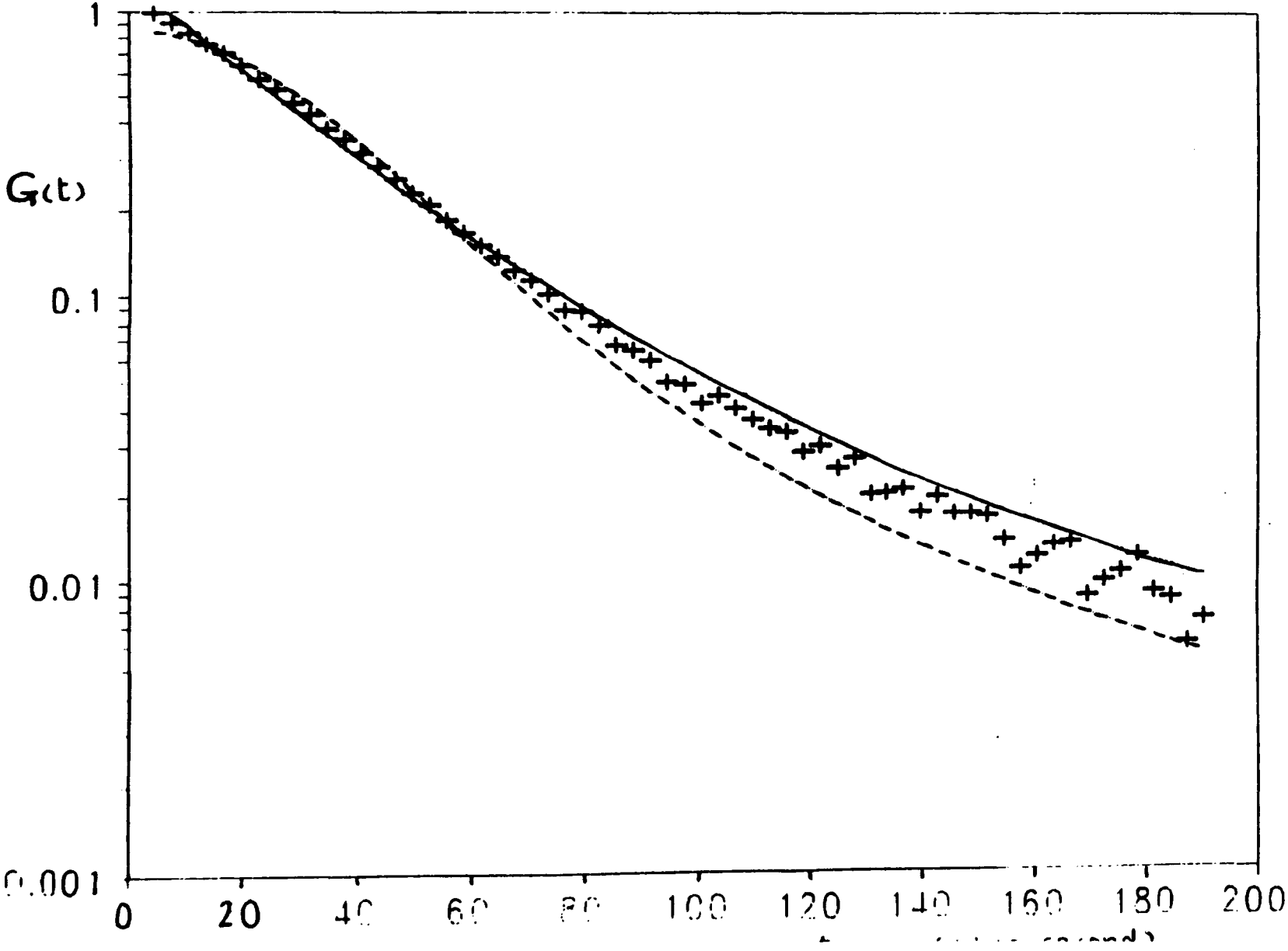

Fig. 2.

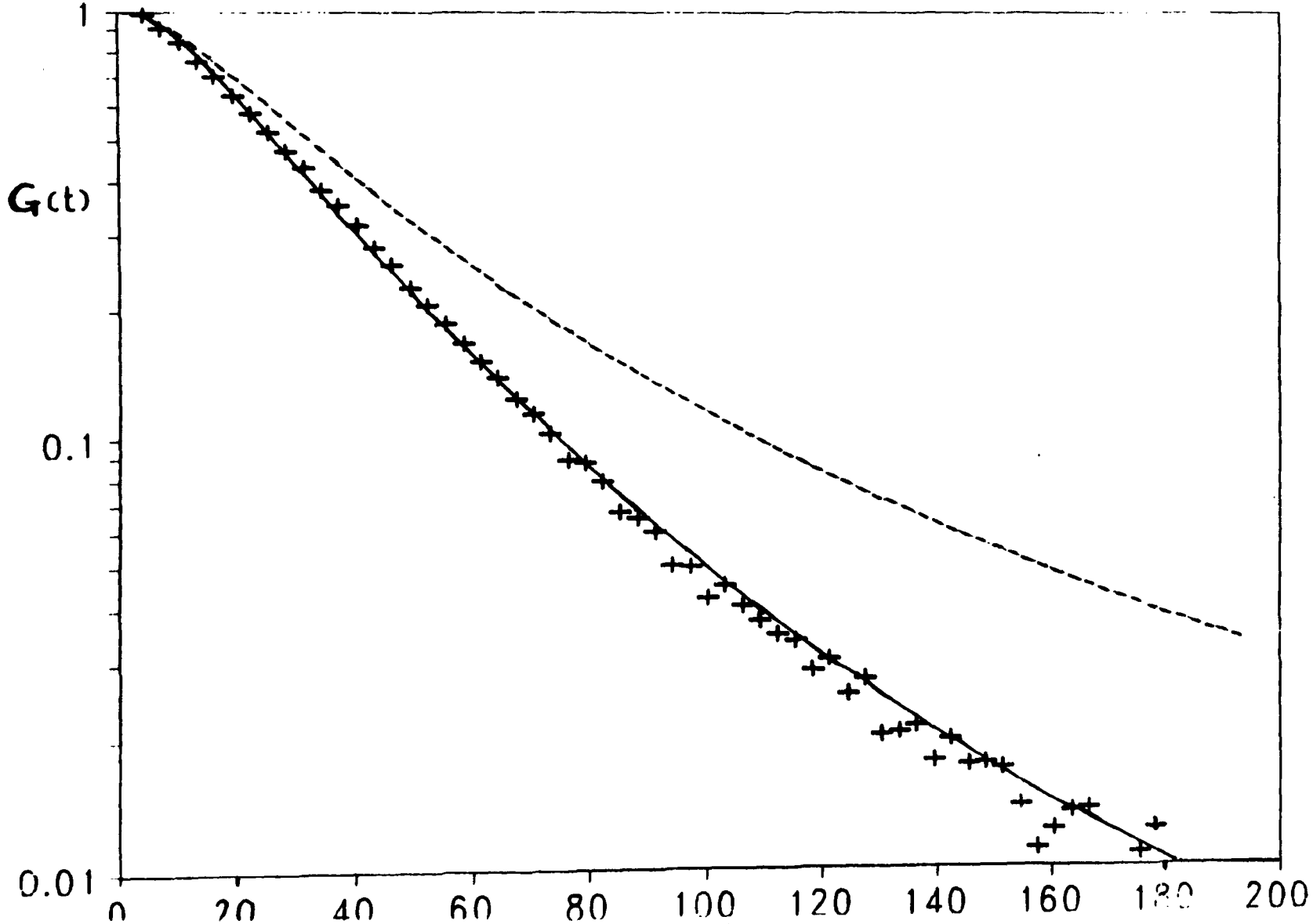

Fig. 2. inset

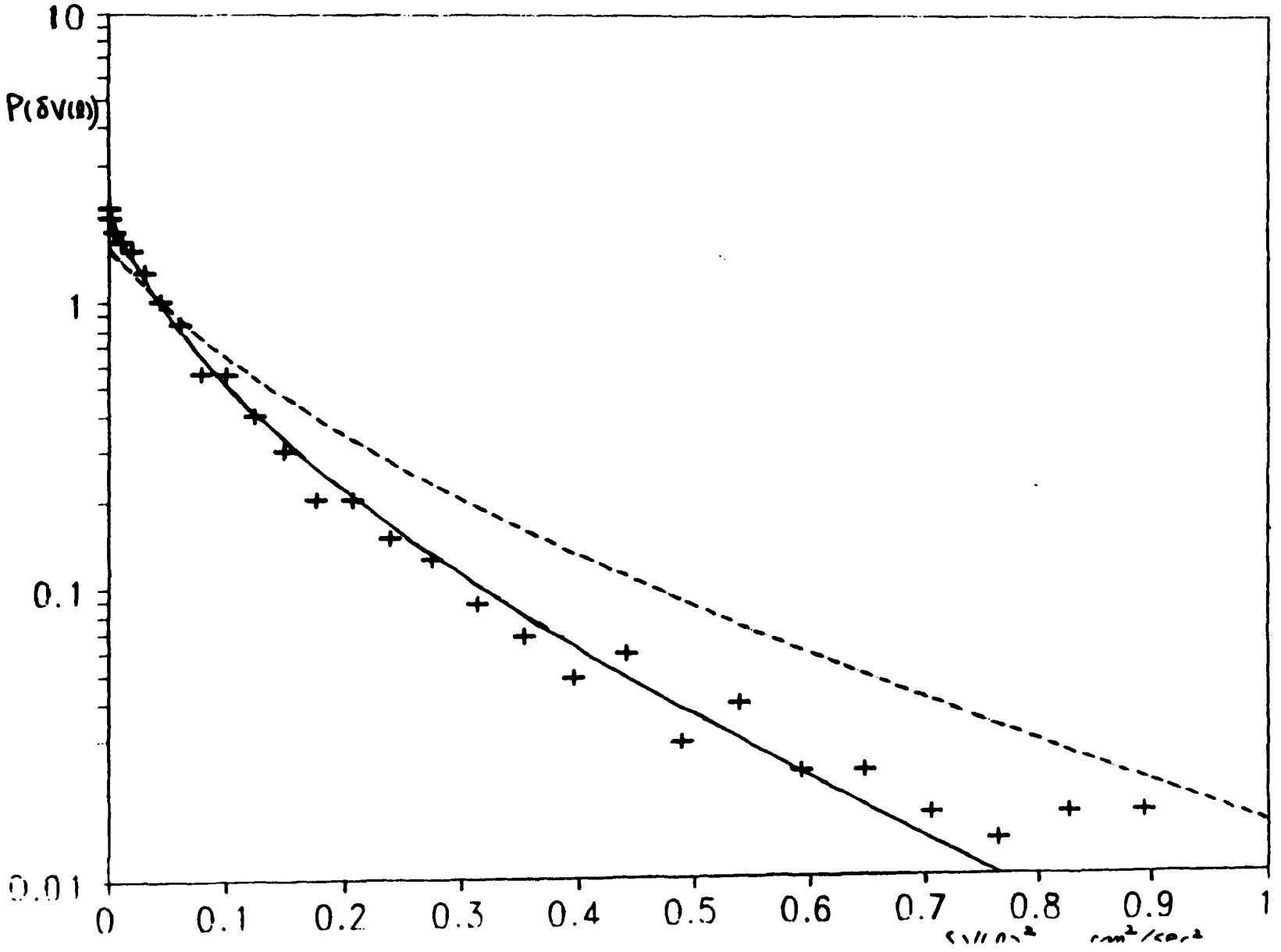

Fig. 3.